

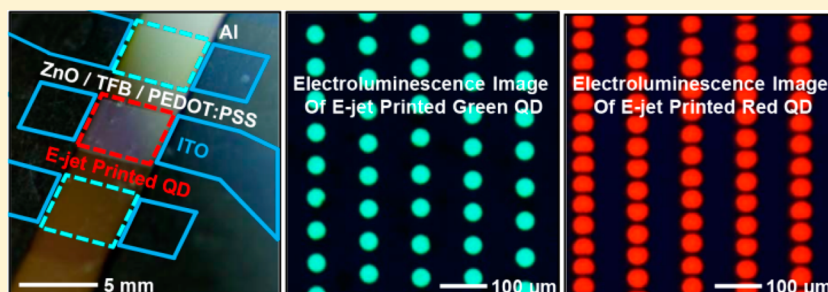
## High-Resolution Patterns of Quantum Dots Formed by Electrohydrodynamic Jet Printing for Light-Emitting Diodes

Bong Hoon Kim,<sup>†</sup> M. Serdar Onses,<sup>‡</sup> Jong Bin Lim,<sup>†</sup> Sooji Nam,<sup>†</sup> Nuri Oh,<sup>†</sup> Hojun Kim,<sup>†</sup> Ki Jun Yu,<sup>†</sup> Jung Woo Lee,<sup>†</sup> Jae-Hwan Kim,<sup>†</sup> Seung-Kyun Kang,<sup>†</sup> Chi Hwan Lee,<sup>†</sup> Jungyup Lee,<sup>†</sup> Jae Ho Shin,<sup>†</sup> Nam Heon Kim,<sup>†</sup> Cecilia Leal,<sup>†</sup> Moonsub Shim,<sup>†</sup> and John A. Rogers<sup>\*,†</sup>

<sup>†</sup>Department of Materials Science and Engineering, Beckman Institute for Advanced Science and Technology, Frederick Seitz Materials Research Laboratory, University of Illinois at Urbana–Champaign, Urbana, Illinois 61801, United States

<sup>‡</sup>Departments of Materials Science and Engineering, Nanotechnology Research Center (ERNAM) Erciyes University, Kayseri, 38039, Turkey

### S Supporting Information



**ABSTRACT:** Here we demonstrate materials and operating conditions that allow for high-resolution printing of layers of quantum dots (QDs) with precise control over thickness and submicron lateral resolution and capabilities for use as active layers of QD light-emitting diodes (LEDs). The shapes and thicknesses of the QD patterns exhibit systematic dependence on the dimensions of the printing nozzle and the ink composition in ways that allow nearly arbitrary, systematic control when exploited in a fully automated printing tool. Homogeneous arrays of patterns of QDs serve as the basis for corresponding arrays of QD LEDs that exhibit excellent performance. Sequential printing of different types of QDs in a multilayer stack or in an interdigitated geometry provides strategies for continuous tuning of the effective, overall emission wavelengths of the resulting QD LEDs. This strategy is useful to efficient, additive use of QDs for wide ranging types of electronic and optoelectronic devices.

**KEYWORDS:** Electrohydrodynamic jet printing, nanopatterning, quantum dots, light-emitting diode, electroluminescence

Colloidal quantum dots (QDs) are nanoscale crystals of semiconducting materials that can be synthesized and processed using bulk solution phase techniques.<sup>1–7</sup> The size-dependent electrical/optical properties of QDs can be exploited in unusual classes of electronic and optoelectronic devices with potential for use in solid-state lighting,<sup>8,9</sup> information displays,<sup>10–15</sup> imaging detectors, and other systems.<sup>16</sup> Quantum-dot based light-emitting diodes (QD LEDs) are of particular interest due to their wide-range color tunability, high brightness, and narrow emission bandwidth.<sup>17–19</sup> Challenges remain, however, in achieving optimized control of charge transport/light emission and in forming the necessary multilayer device structures.<sup>20,21</sup> Research over the last several years has led to significant progress on the former set of topics.<sup>22</sup> Approaches to address the latter include conventional ink jet printing,<sup>23</sup> advanced techniques of transfer printing<sup>12,24,25</sup> and, in initial feasibility demonstrations, dip pen nanolithography.<sup>26–28</sup> The aim is to enable patterning/stacking of red-green-blue (RGB) QDs into high-resolution, pixelated geometries with accurate control of registration, efficient utilization of the materials, and

minimal chemical contamination. Here, we present a high-resolution, additive nanofabrication technique that exploits controlled, electrohydrodynamic ejection of fluids through fine nozzles for the patterned delivery of QDs to a target substrate.<sup>29</sup> The method is similar in terms of its additive nature, compatibility with multiple material “inks”, and programmable definition of pattern layouts (i.e., maskless operation) to conventional inkjet techniques, but it offers levels of resolution, registration, and thickness control that are vastly superior. This electrohydrodynamic jet (e-jet) printing procedure<sup>30–32</sup> also does not require prepatterned topographical or chemical patterns to guide material flows. Previous work demonstrates compatibility with a wide variety of inks, ranging from carbon nanotubes (CNTs)<sup>33</sup> to proteins and DNA,<sup>34,35</sup> to block copolymers,<sup>36,37</sup> conducting polymers and many others. The work reported here establishes versatile capabilities when used with solution suspensions of QDs,

**Received:** October 1, 2014

**Revised:** December 28, 2014

**Published:** January 13, 2015

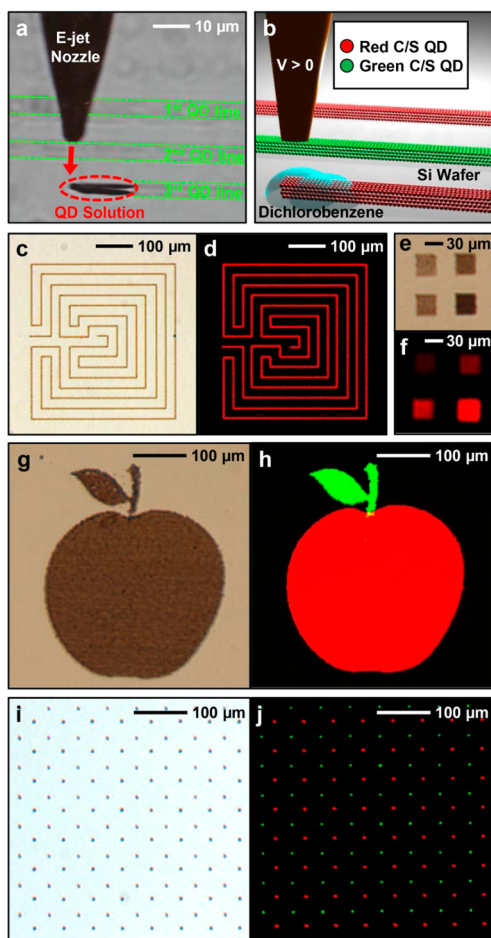


**Figure 1.** Electrohydrodynamic jet printing as a route to high-resolution patterns of QDs. (a) An optical microscope image of a metal-coated glass nozzle ( $5\ \mu\text{m}$  internal diameter at the tip) and a target substrate during the printing process. (b) Schematic illustration corresponding to the image of (a). The inks consist of a dilute solutions (0.25%) of different types of QDs (CdSe/CdZnSeS green or CdSe/CdS/ZnS red core/shell QDs) in dichlorobenzene. The solvent evaporates during and immediately after printing. (c,d) QDs printed in linear geometries: (c) optical and (d) fluorescence images of a pattern generated in a continuous printing mode. (e,f) QDs printed into filled square geometries: (e) optical and (f) fluorescence images of an array of squares ( $30 \times 30\ \mu\text{m}^2$ ) formed by raster scanning in the continuous mode. The spacings between adjacent lines decreases from top left to bottom right. (g,h) QDs printed into complex shapes: (g) optical and (h) composite fluorescence images of a pattern of red and green QDs printed in a raster scanning mode to obtain a uniform coverage. (i,j) QDs printed into arrays of spots: (i) optical and (j) composite fluorescence images of arrays of red and green QDs printed in a drop on demand mode. Nozzles with internal diameters of 2 and  $5\ \mu\text{m}$  were used in the results presented above.

through demonstrations of wide-ranging, multicolored patterns of QDs in various geometries. Such printed structures can be incorporated into functional QD LEDs with expected properties. Unusual printed device configurations such as vertical stacks of QDs enable LEDs with visible light emission at tailored wavelengths.

Figure 1 demonstrates the ability of e-jet printing to form diverse patterns of multiple types of QDs with good registration. Here, solutions of QDs (CdSe/CdZnSeS green or CdSe/CdS/ZnS red core/shell QDs)<sup>38,39</sup> in organic solvents (dichlorobenzene) serve as the inks (Supporting Information 1).

A voltage bias applied between a substrate and a metal-coated glass capillary induces rapid flow of the ink through the fine opening (e.g.,  $5\ \mu\text{m}$ ) at the end of the nozzle (Figure 1a,b and Supporting Information 2). The simultaneous programmed movement of the substrate and control of the voltage enables patterned delivery of QDs in nearly any geometry. Line patterns can be efficiently created by operating the e-jet system in a mode that involves ink delivery in the form of a single, continuous jet, as shown in Figure 1c,d. In a raster scanning operation with this mode, QDs can be printed as filled solid patterns (e.g., squares of  $30 \times 30\ \mu\text{m}^2$ ) as in Figure 1e,f. The spacings between adjacent printed lines, or the number of overlaid printing sequences can be varied to control the thicknesses of the patterns without significant change in the lateral dimensions. Increases in thickness manifest as increased fluorescence (Figure 1f). Filled polygons with complex geometries can be designed by converting an image to numerical commands for automated printing. Different QDs can be delivered with precise registration to different regions of a single pattern. Figure 1g,h presents an example of a printed cartoon image of an apple formed with green and red QDs. The strong, spatially uniform patterns of fluorescence suggest full area coverage and uniform thickness across the pattern. In a pulsatile mode, e-jet printing yields arrays of circular deposits of QDs with diameters of  $\sim 3.9\ \mu\text{m}$  (Figure 1i,j), using drop-on-demand operation. Here, control over the number of delivered droplets determines the thickness of the printed materials.

Patterning QDs with precise control of their thicknesses and nanoscale lateral dimensions represent two critical capabilities for advanced applications. The thickness can be controlled through a combination of printing parameters including the size of the nozzle, the stage speed, ink composition, and voltage bias (Supporting Information 3). As an example, Figure 2a–c shows printed lines of QDs where different nozzles provide access to different thicknesses. Here thicknesses evaluated at the center of the lines and their average widths are  $140\ \text{nm}$ ,  $70\ \text{nm}$ ,  $25\ \text{nm}$ , and  $1.8\ \mu\text{m}$ ,  $1.2\ \mu\text{m}$ ,  $0.25\ \mu\text{m}$ , respectively. The thickness of a line can be adjusted, without significant change in the width, through control of the speed of the stage. The dependence of thickness on stage speed appears in Figure 2d. In addition to precise control of thickness, e-jet allows patterning with submicron resolution and large area coverage, as shown for the case of a line with average width  $\sim 410\ \text{nm}$  and length of tens of microns. QDs form close-packed structures with full area coverage within such patterns (Figure 2e). The line width variation is typically  $\sim 30\ \text{nm}$  (Figure 2f), due to uncontrolled interactions between the ink and the substrate during the drying process and by the intrinsic, particulate nature of the material. Prepatterned topographical and/or chemical structures on the substrate could further reduce such variations.

Rectangular/square patterns of QDs represent basic geometries for use in displays. The thickness of the QD layer critically determines the electro-optical performance of a QD LED.<sup>13,15</sup> Figure 2g and h present AFM images of two different squares with average thicknesses of  $18 \pm 10$  and  $33 \pm 7\ \text{nm}$  generated in the continuous jet mode with two different choices for spacings between adjacent lines during the raster scanning process. Figure 2i shows a cross-sectional height profile of the square (roughness  $\sim 7\ \text{nm}$ ). The roughness typically increases at thicknesses that correspond to a few layers of QDs. Improvements in this regime may be possible by adjusting the ink compositions (e.g., using mixtures of solvents<sup>40</sup>) or by postprocessing of the films (e.g., solvent annealing<sup>41</sup>).



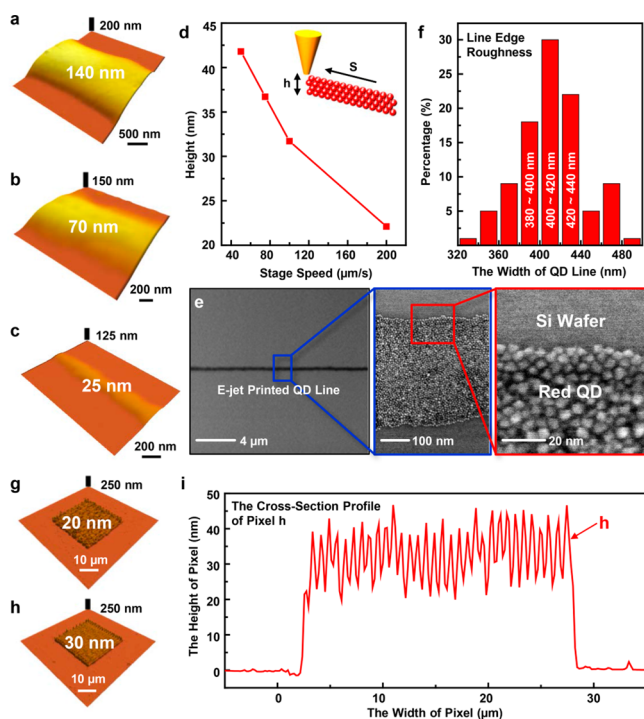


**Figure 2.** Precise control of the sizes and thicknesses of patterns of QDs formed by e-jet printing. (a–c) AFM images of QDs printed into lines with different thicknesses. The text over the images indicates the thickness at the center of the lines. Lines printed using a nozzle with an internal diameter of (a) 5  $\mu\text{m}$ , (b) 2  $\mu\text{m}$ , and (c) 1  $\mu\text{m}$ . (d) Plot of the heights at the centers of the lines as a function of the stage speed. The printing used a nozzle with 1  $\mu\text{m}$  internal diameter. (e) SEM images of a  $\sim 400$  nm wide line pattern printed using a nozzle with 1  $\mu\text{m}$  internal diameter. The images at the right present high-magnification views of the line. (f) Images that highlight the edge roughness associated with a  $\sim 400$  nm wide printed line. (g,h) AFM images of square pads printed using a nozzle with 2  $\mu\text{m}$  internal diameter. The thickness of the squares was varied by changing the spacing between adjacent printed lines. (i) Cross-sectional height profiles obtained from the AFM images shown in part h.

Figure 3a,b shows schematic illustrations and images of QD LEDs formed with e-jet printed patterns of QDs. These devices incorporate (i) indium tin oxide (ITO; on a glass substrate) as the anode layer, (ii) poly(ethylenedioxythiophene)/poly(styrenesulfonate) (PEDOT/PSS) as the hole injection layer (HIL), (iii) poly[(9,9-dioctylfluorenyl-2,7-diyl)-*co*-(4,4-(N-(4-*s*-butylphenyl)) diphenylamine)] (TFB) as the hole transport layer (HTL), (iv) CdSe/CdZnSeS green QDs or CdSe/CdS/ZnS red QDs for emission, (v) ZnO as the electron transport layer (ETL), and (vi) electron-beam evaporated Al as the cathode layer.<sup>42</sup> Figure 3c,d presents images of the electroluminescence from e-jet printed green and red QD LEDs, respectively. The emission properties can be controlled through the stage speed (50  $\mu\text{m}/\text{s}$  and 30  $\mu\text{m}/\text{s}$  for green and red QD LED, respectively) and the distance between the QD dot patterns. Figure 3e–h shows the current density–voltage ( $J$ – $V$ ), luminance–voltage ( $L$ – $V$ ), and the external quantum efficiency (EQE) of a typical green and red LED with spatially uniform layers of QDs. The maximum luminance and EQE of green QD LED are 36 000  $\text{cd}/\text{m}^2$  and 2.5%, respectively (see Supporting Information 4 for current and power efficiency graph). The results are on par with the best reported performances of QD LEDs of the same device structure fabricated

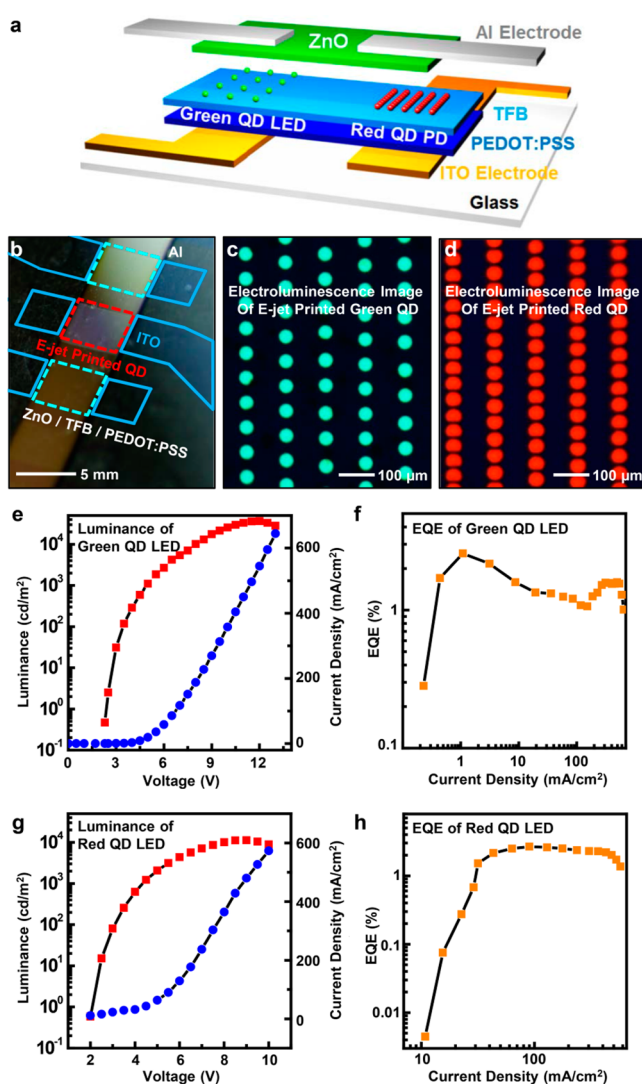


**Figure 3.** E-jet printed homogeneous QD array for QD LEDs. (a,b) Schematic description and photograph of QDs LEDs. (c,d) Optical micrographs of electroluminescence of green and red QD LEDs. Each QD pattern was precisely printed using different stage speeds (50  $\mu\text{m}/\text{s}$  for green QDs and 30  $\mu\text{m}/\text{s}$  for red QDs, respectively). Plots of current density–voltage ( $J$ – $V$ ) and luminance–voltage ( $L$ – $V$ ) (e,g) and the external quantum efficiency (EQE) (f,h) of green and red QD LED. A square pad of QDs with uniform thickness (pixel size: 1 mm  $\times$  1 mm) defined by e-jet printing was used to analyze the device performance.

by spin-casting and/or vacuum deposition techniques.<sup>12,43</sup> The maximum luminance and EQE of red QD LED are 11 250  $\text{cd}/\text{m}^2$  and 2.6%, respectively.

Figure 4a,b provides a schematic illustration of a QD LED that incorporates a printed array of QDs stacked and patterned heterogeneously, as the active layer. Type I (Figure 4a) and II (Figure 4b) devices correspond to “array of lines of green QDs on a uniform spin-coated film of red QDs” and “array of alternating dots of green and red QDs”, respectively. All other layers (anode, HIL, HTL, ETL, and cathode) of these devices are identical to those of the structure in Figure 3a. Figure 4c–f presents fluorescence images and photographs of Type I and Type II devices operating at 4 V. The array of yellow lines corresponds to the areas of overlap between the green and red QDs (Figure 4c). Alternating green and red dots are apparent against the black background as in Figure 4d.

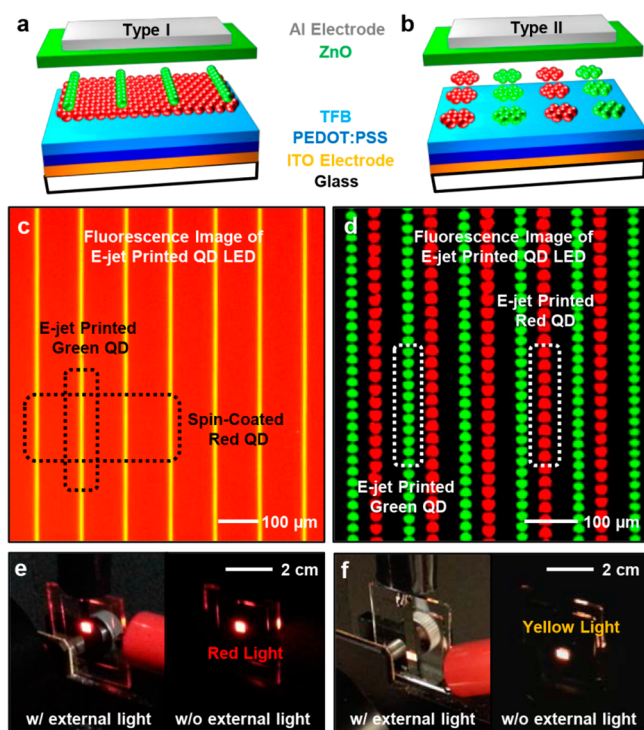


**Figure 4.** E-jet printed heterogeneous QD array for QD LEDs of type I and II designation. (a,b) Schematic illustrations of QD LEDs of type I and II with heterogeneously stacked/patterned QD arrays formed by e-jet printing, as the active layers. (c,d) Composite fluorescence images of QD LEDs. In the type I device, the red QD thin film was spin-cast on the stack of TFB, PEDOT/PSS, and micropatterned ITO electrode. The line array of green QDs was then formed by e-jet printing. In the type II device, green and red QDs in the form of arrays of dot were alternatively printed on the same stack. (e,f) Photographs of QD LEDs of type I and II designation, operating at 4 V.

The devices appear red (Figure 4e) and yellow (Figure 4f) to the unaided eye.

Figure 5a–d shows the normalized electroluminescence (EL) spectra of QD LEDs with the Type I and Type II configurations. The individual EL emission from each QD layer can be clearly observed in both systems; however, in type I, the green emission is suppressed relative to the red (Figure 5a). This behavior likely arises from some combination of (i) energy transfer from green to red QDs in this stack, and (ii) higher electrical resistance, and corresponding lower injected current, in the green/red stack compared to that of the red film. The maximum of the normalized green and red EL appears in the voltage-resolved measurements of Figure 5b. The normalized EL spectra of Type II devices appear in Figure 5c. As might be expected, here the intensities for green and red light are comparable (Figure 5d).

This paper demonstrates that advanced techniques in e-jet printing offer powerful capabilities in patterning QD materials from solution inks, over large areas. Various homogeneous QD patterns, for example, dot, line, square, and complex images, are readily possible, with tunable dimensions and thickness. Moreover, these arrays as well as those constructed with multiple different QD materials, directly patterned/stacked by e-jet printing, can be utilized as photoluminescent and electroluminescent layers. These capabilities also suggest possibilities in all-QD-based printed electronic systems that could combine QD transistors,<sup>44–48</sup> QD solar cells,<sup>49–54</sup> QD downconverters,<sup>55</sup> QD photodetectors,<sup>56,57</sup>

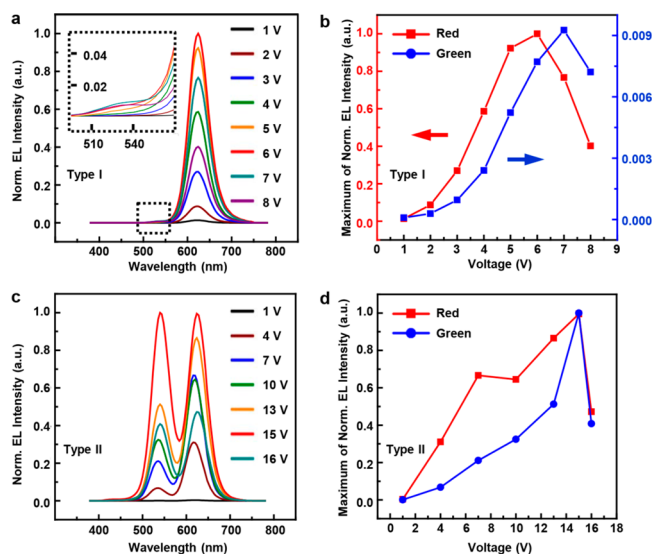


**Figure 5.** EL properties of heterogeneously e-jet printed QD LEDs with type I and II designs. Plots of normalized EL spectra of QD LEDs with type I (a,b) and II (c,d) designs.

and QD LEDs on a common substrate. This strategy also has strong potential for integration of QD patterns into functional semiconducting thin films or with other kinds of printable nanomaterials, for example, CNT, graphene, and DNA. Exploring these directions as well as furthering the engineering development of the basic methodologies are topics of current work.

## ■ ASSOCIATED CONTENT

### Supporting Information

Details of the quantum dot synthesis, e-jet printer, experimental conditions for e-jet printing, and current and power efficiency of e-jet printed green and red QD LEDs are given in this section. This material is available free of charge via the Internet at <http://pubs.acs.org>.

## ■ AUTHOR INFORMATION

### Corresponding Author

\*E-mail: [jrogers@illinois.edu](mailto:jrogers@illinois.edu).

### Author Contributions

B.H.K. and M.S.O. contributed equally in this manuscript.

### Notes

The authors declare no competing financial interest.

## ■ ACKNOWLEDGMENTS

This material is based on work supported by the Dow Chemical Company and the Air Force Research Laboratory (AFRL).

## ■ REFERENCES

- (1) Yin, Y.; Talapin, D. *Chem. Soc. Rev.* **2013**, *42*, 2484.
- (2) Talapin, D. V. *MRS Bull.* **2012**, *37*, 63.
- (3) Norris, D. J.; Efros, A. L.; Erwin, S. C. *Science* **2008**, *319*, 1776.
- (4) Cargnello, M.; Doan-Nguyen, V. V. T.; Gordon, T. R.; Diaz, R. E.; Stach, E. A.; Gorte, R. J.; Fornasiero, P.; Murray, C. B. *Science* **2013**, *341*, 771.
- (5) Shevchenko, E. V.; Talapin, D. V.; Kotov, N. A.; O'Brien, S.; Murray, C. B. *Nature* **2006**, *439*, 55.
- (6) Talapin, D. V.; Shevchenko, E. V.; Bodnarchuk, M. I.; Ye, X.; Chen, J.; Murray, C. B. *Nature* **2009**, *461*, 964.
- (7) Urban, J. J.; Talapin, D. V.; Shevchenko, E. V.; Kagan, C. R.; Murray, C. B. *Nat. Mater.* **2007**, *6*, 115.

- (8) Demir, H. V.; Nizamoglu, S.; Erdem, T.; Mutlugun, E.; Gaponik, N.; Eychmüller, A. *Nano Today* **2011**, *6*, 632.
- (9) Ziegler, J.; Xu, S.; Kucur, E.; Meister, F.; Batentschuk, M.; Gindele, F.; Nann, T. *Adv. Mater.* **2008**, *20*, 4068.
- (10) Jang, E.; Jun, S.; Jang, H.; Lim, J.; Kim, B.; Kim, Y. *Adv. Mater.* **2010**, *22*, 3076.
- (11) Pal, B. N.; Ghosh, Y.; Brovelli, S.; Laocharoensuk, R.; Klimov, V. I.; Hollingsworth, J. A.; Htoon, H. *Nano Lett.* **2012**, *12*, 331.
- (12) Kim, T.-H.; Cho, K.-S.; Lee, E. K.; Lee, S. J.; Chae, J.; Kim, J. W.; Kim, D. H.; Kwon, J.-Y.; Amaratunga, G.; Lee, S. Y.; Choi, B. L.; Kuk, Y.; Kim, J. M.; Kim, K. *Nat. Photonics* **2011**, *5*, 176.
- (13) Qian, L.; Zheng, Y.; Xue, J.; Holloway, P. H. *Nat. Photonics* **2011**, *5*, 543.
- (14) Kwak, J.; Bae, W. K.; Lee, D.; Park, I.; Lim, J.; Park, M.; Cho, H.; Woo, H.; Yoon, D. Y.; Char, K.; Lee, S.; Lee, C. *Nano Lett.* **2012**, *12*, 2362.
- (15) Mashford, B. S.; Stevenson, M.; Popovic, Z.; Hamilton, C.; Zhou, Z.; Breen, C.; Steckel, J.; Bulovic, V.; Bawendi, M.; Coe-Sullivan, S.; Kazlas, P. T. *Nat. Photonics* **2013**, *7*, 407.
- (16) Michalet, X.; Pinaud, F. F.; Bentolila, L. A.; Tsay, J. M.; Doose, S.; Li, J. J.; Sundaresan, G.; Wu, A. M.; Gambhir, S. S.; Weiss, S. *Science* **2005**, *307*, 538.
- (17) Kim, J. Y.; Voznyy, O.; Zhitomirsky, D.; Sargent, E. H. *Adv. Mater.* **2013**, *25*, 4986.
- (18) Talapin, D. V.; Lee, J.-S.; Kovalenko, M. V.; Shevchenko, E. V. *Chem. Rev.* **2010**, *110*, 389.
- (19) Saboktakin, M.; Ye, X.; Oh, S. J.; Hong, S.-H.; Fafarman, A. T.; Chettiar, U. K.; Engheta, N.; Murray, C. B.; Kagan, C. R. *ACS Nano* **2012**, *6*, 8758.
- (20) Caruge, J. M.; Halpert, J. E.; Wood, V.; Bulović, V.; Bawendi, M. G. *Nat. Photonics* **2008**, *2*, 247.
- (21) Lee, J.-S.; Kovalenko, M. V.; Huang, J.; Chung, D. S.; Talapin, D. V. *Nat. Nanotechnol.* **2011**, *6*, 348.
- (22) Shirasaki, Y.; Supran, G. J.; Bawendi, M. G.; Bulović, V. *Nat. Photonics* **2013**, *7*, 13.
- (23) Wood, V.; Panzer, M. J.; Chen, J.; Bradley, M. S.; Halpert, J. E.; Bawendi, M. G.; Bulovic, V. *Adv. Mater.* **2009**, *21*, 1.
- (24) Kim, T.-H.; Chung, D.-Y.; Ku, J.; Song, I.; Sul, S.; Kim, D.-H.; Cho, K.-S.; Choi, B. L.; Kim, J. M.; Hwang, S.; Kim, K. *Nat. Commun.* **2013**, *4*, 1.
- (25) Kim, L.; Anikeeva, P. O.; Coe-Sullivan, S. A.; Steckel, J. S.; Bawendi, M. G.; Bulovic, V. *Nano Lett.* **2008**, *8*, 4513.
- (26) Gokarna, A.; Lee, S.-K.; Hwang, J.-S.; Cho, Y.-H. *J. Korean Phys. Soc.* **2008**, *53*, 3047.
- (27) Wang, Y.; Zhang, Y.; Li, B.; Lü, J.; Hu, J. *Appl. Phys. Lett.* **2007**, *90*, 133102.
- (28) Roy, D.; Munz, M.; Colombi, P.; Bhattacharyya, S.; Salvétat, J.-P.; Cumpson, P. J.; Saboungi, M.-L. *Appl. Surf. Sci.* **2007**, *254*, 1394.
- (29) Kress, S. J. P.; Richner, P.; Jayanti, S. V.; Galliker, P.; Kim, D. K.; Poulidakos, D.; Norris, D. J. *Nano Lett.* **2014**, DOI: 10.1021/nl5026997.
- (30) Park, J.-U.; Lee, S.; Unarunotai, S.; Sun, Y.; Dunham, S.; Song, T.; Ferreira, P. M.; Alleyne, A. G.; Paik, U.; Rogers, J. A. *Nano Lett.* **2010**, *10*, 584.
- (31) Song, C. H.; Back, S. Y.; Yu, S.; Lee, H. J.; Kim, B. S.; Yang, N. Y.; Jeong, S. H.; Ahn, H. *J. Nanosci. Nanotechnol.* **2012**, *12*, 475.
- (32) Back, S. Y.; Song, C. H.; Yu, S.; Lee, H. J.; Kim, B. S.; Yang, N. Y.; Jeong, S. H.; Ahn, H. *J. Nanosci. Nanotechnol.* **2012**, *12*, 446.
- (33) Park, J.-U.; Hardy, M.; Kang, S. J.; Barton, K.; Adair, K.; Mukhopadhyay, D. K.; Lee, C. Y.; Strano, M. S.; Alleyne, A. G.; Georgiadis, J. G.; Ferreira, P. M.; Rogers, J. A. *Nat. Mater.* **2007**, *6*, 782.
- (34) Shigeta, K.; He, Y.; Sutanto, E.; Kang, S.; Le, A.-P.; Nuzzo, R. G.; Alleyne, A. G.; Ferreira, P. M.; Lu, Y.; Rogers, J. A. *Anal. Chem.* **2012**, *84*, 10012.
- (35) Park, J.-U.; Lee, J. H.; Paik, U.; Lu, Y.; Rogers, J. A. *Nano Lett.* **2008**, *8*, 4210.
- (36) Onses, M. S.; Song, C.; Williamson, L.; Sutanto, E.; Ferreira, P. M.; Alleyne, A. G.; Nealey, P. F.; Ahn, H.; Rogers, J. A. *Nat. Nanotechnol.* **2013**, *8*, 667.
- (37) Onses, M. S.; Ramírez-Hernández, A.; Hur, S.-M.; Sutanto, E.; Williamson, L.; Alleyne, A. G.; Nealey, P. F.; de Pablo, J. J.; Rogers, J. A. *ACS Nano* **2014**, *8*, 6606.
- (38) Bae, W. K.; Kwak, J.; Park, J. W.; Char, K.; Lee, C.; Lee, S. *Adv. Mater.* **2009**, *21*, 1690.
- (39) Lim, J.; Jun, S.; Jang, E.; Baik, H.; Kim, H.; Cho, J. *Adv. Mater.* **2007**, *19*, 1927.
- (40) Lim, J. A.; Lee, W. H.; Lee, H. S.; Lee, J. H.; Park, Y. D.; Cho, K. *Adv. Funct. Mater.* **2008**, *18*, 229.
- (41) Xiong, Z.; Liu, C. *Org. Electron.* **2012**, *13*, 1532.
- (42) Oh, N.; Nam, S.; Zhai, Y.; Deshpande, K.; Trefonas, P.; Shim, M. *Nat. Commun.* **2014**, *5*, 3642.
- (43) Cho, K.-S.; Lee, E. K.; Joo, W.-J.; Jang, E.; Kim, T.-H.; Lee, S. J.; Kwon, S.-J.; Han, J. Y.; Kim, B.-K.; Choi, B. L.; Kim, J. M. *Nat. Photonics* **2009**, *3*, 341.
- (44) Oh, S. J.; Berry, N. E.; Choi, J.-H.; Gaubling, E. A.; Lin, H.; Paik, T.; Diroll, B. T.; Muramoto, S.; Murray, C. B.; Kagan, C. R. *Nano Lett.* **2014**, *14*, 1559.
- (45) Oh, S. J.; Berry, N. E.; Choi, J.-H.; Gaubling, E. A.; Paik, T.; Hong, S.-H.; Murray, C. B.; Kagan, C. R. *ACS Nano* **2013**, *7*, 2413.
- (46) Kim, D. K.; Lai, Y.; Diroll, B. T.; Murray, C. B.; Kagan, C. R. *Nat. Commun.* **2012**, *3*, 1.
- (47) Talapin, D. V.; Murray, C. B. *Science* **2005**, *310*, 86.
- (48) Kang, M. S.; Sahu, A.; Norris, D. J.; Frisbie, C. D. *Nano Lett.* **2010**, *10*, 3727.
- (49) Chuang, C.-H. M.; Brown, P. R.; Bulovic, V.; Bawendi, M. G. *Nat. Mater.* **2014**, *13*, 796.
- (50) Brown, P. R.; Kim, D.; Lunt, R. R.; Zhao, N.; Bawendi, M. G.; Grossman, J. C.; Bulovic, V. *ACS Nano* **2014**, *8*, 5863.
- (51) Zhao, N.; Osedach, T. P.; Chang, L.-Y.; Geyer, S. M.; Wanger, D.; Binda, M. T.; Arango, A. C.; Bawendi, M. G.; Bulovic, V. *ACS Nano* **2010**, *4*, 3743.
- (52) Leschkie, K. S.; Beatty, T. J.; Kang, M. S.; Norris, D. J.; Aydil, E. S. *ACS Nano* **2009**, *3*, 3638.
- (53) Panthani, M. G.; Kurley, J. M.; Crisp, R. W.; Dietz, T. C.; Ezzyat, T.; Luther, J. M.; Talapin, D. V. *Nano Lett.* **2013**, *14*, 670.
- (54) Tisdale, W. A.; Williams, K. J.; Timp, B. A.; Norris, D. J.; Aydil, E. S.; Zhu, X.-Y. *Science* **2010**, *328*, 1543.
- (55) Song, W.-S.; Kim, J.-H.; Yang, H. *Mater. Lett.* **2013**, *111*, 104.
- (56) Prins, F.; Buscema, M.; Seldenthuis, J. S.; Etaki, S.; Buchs, G.; Barkelid, M.; Zwiller, V.; Gao, Y.; Houtepen, A. J.; Siebbeles, L. D. A.; van der Zant, H. S. J. *Nano Lett.* **2012**, *12*, 5740.
- (57) Sarasqueta, G.; Choudhury, K. R.; Subbiah, J.; So, F. *Adv. Funct. Mater.* **2011**, *21*, 167.